



Repositorio Institucional de la Universidad Autónoma de Madrid

<https://repositorio.uam.es>

Esta es la **versión de autor** del artículo publicado en:

This is an **author produced version** of a paper published in:

Fuel Processing Technology 118 (2014): 148-155

DOI: <https://doi.org/10.1016/j.fuproc.2013.08.019>

Copyright: © 2013 Elsevier B.V. All rights reserved.

El acceso a la versión del editor puede requerir la suscripción del recurso

Access to the published version may require subscription

PREPARATION OF GRANULAR ACTIVATED CARBONS FROM GRAPE SEEDS BY CYCLES OF LIQUID PHASE OXIDATION AND THERMAL DESORPTION

Diana Jimenez-Cordero, Francisco Heras, Noelia Alonso-Morales, Miguel A. Gilarranz, Juan J. Rodríguez*

S.D. Ingeniería Química. Universidad Autónoma de Madrid.
Ctra. Colmenar Viejo, km 15. 28049 Madrid (Spain)

Abstract

Activation of grape seeds char upon successive cycles of liquid phase oxidation followed by high-temperature desorption permits a tailored development of porosity. In this work three different oxidants (HNO_3 , H_2O_2 , $(\text{NH}_4)_2\text{S}_2\text{O}_8$), have been tested and the desorption temperature has been varied within 850-950°C upon 10 activation cycles. A high increase of BET surface area was observed in the first five cycles with HNO_3 as oxidizing agent giving rise to values higher than $1200\text{m}^2\text{g}^{-1}$ at around 50% burn-off. Activation with H_2O_2 and $(\text{NH}_4)_2\text{S}_2\text{O}_8$ led to a significantly lower development of surface area, with 600 and $800\text{m}^2\text{g}^{-1}$ respectively at that burn-off. The analysis of the pore size distribution showed that porosity was generated through the creation of new micropores and widening of existing ones upon activation with HNO_3 and $(\text{NH}_4)_2\text{S}_2\text{O}_8$, whereas H_2O_2 mostly led to the widening of the narrow micropores already existing in the starting char. The activated carbons obtained are essentially microporous, with some small contribution of mesoporosity in the HNO_3 series ($V_{\text{micro}}=0.69\text{cm}^3\text{g}^{-1}$; $V_{\text{meso}}=0.07\text{cm}^3\text{g}^{-1}$). SEM images showed that the activated carbons maintained the granular morphology of the seeds after 10 cycles showing a hollow core structure with a wall thickness of about $200\mu\text{m}$.

* Corresponding author Tel.: +34 914978051; fax: +34 914972981.

E-mail address: fran.heras@uam.es

Keywords: Grape seeds; Cyclic activation; Granular activated carbon; Liquid phase oxidation.

1. Introduction

Activation by cyclic oxygen chemisorption-desorption allows the preparation of porous carbons with tailored development of porosity for targeted applications [1, 3]. The method consists of an oxidation stage under conditions that promote oxygen uptake by chemisorption, usually at relatively low temperature, followed by desorption in an inert atmosphere at high temperature [4]. This chemisorptions step permits a better control of porosity development while the desorption step involves partial gasification of carbon, thus leading to burn-off. The sequence can be repeated until convenient porosity development is achieved. This method provides an efficient way to create porosity from a precursor and to controllably modify the porous structure of a carbonaceous material while maintaining the physical integrity of the particle [5].

We have used cyclic activation of grape seeds char with oxygen as oxidizing agent in previous works [5] with interesting and promising results. The best results were obtained at chemisorption temperatures between 200 and 300°C. Depending on the chemisorption and desorption temperature the burn-off per cycle ranged between 0.4 and 9.0%. Activated carbons with BET surface areas up to 1300m²g⁻¹ were obtained while maintaining the granular morphology of the precursor even after ten activation cycles. The activated carbons prepared by this procedure were essentially microporous materials. In a former work [6] we reported that the preparation of activated carbons from waste tire char upon successive cycles of oxidation-desorption using nitric acid, hydrogen peroxide and ammonium persulphate as oxidizing agents in liquid phase led

to different patterns in burn-off and porosity development ($\text{HNO}_3 > \text{H}_2\text{O}_2 > (\text{NH}_4)_2\text{S}_2\text{O}_8$). The activated carbons obtained in general showed a well developed mesoporosity. Other authors [7] used the cyclic activation with liquid phase oxidation with H_2O_2 at high pressure and further heat-treatment at 900°C in inert atmosphere to obtain microporous activated carbons from sucrose and cellulose with surface areas of $950\text{-}1600\text{m}^2\text{g}^{-1}$ (DR method from N_2 isotherms) and burn-offs ranging between 18 and 39%, concluding that the method provides materials with suitable textural properties for application in electrochemical capacitors.

The results above indicate the potential of liquid phase oxidation to tune the porosity development in cyclic activation, although the starting material may also be an important factor. In general, liquid phase oxidation is used to modify the surface chemical composition (creating oxygenated functional groups) [6-10] and the porosity of carbon materials, being the oxidants most commonly used nitric acid, hydrogen peroxide or ammonium persulphate [6-17]. Liquid phase oxidation has been mainly used for the modification of commercial activated carbons [6-10] and own-made activated carbon from biomass precursors [11-17]. The extent of the textural changes depends on both the structure of the starting activated carbon and the oxidation treatment. In general, the extent of oxidation follows the order is $\text{HNO}_3 > \text{H}_2\text{O}_2 > (\text{NH}_4)_2\text{S}_2\text{O}_8$ [6, 9, 11, 17]. The higher oxidizing action of HNO_3 is attributed to higher fluidity and greater diffusion in the pores of the activated carbon [14]. In contrast, H_2O_2 and $(\text{NH}_4)_2\text{S}_2\text{O}_8$ suffer from decomposition in aqueous solution and a larger molecular size, which confers a different oxidizing action [14]. In all cases, after oxidation, a decrease in surface area and pore volume of activated carbons is reported, generally explained by the restriction of the pore volume available for N_2 adsorption due to the

formation of oxygen-containing groups at the entrance and/or on the walls of micropores and by the destruction of the pore walls and its collapse when oxygenated terminal groups are created. That is especially the case for HNO_3 oxidation treatment which provokes a severe damage of pore walls [9, 11-13, 16].

Liquid phase oxidation of activated carbons also leads to the formation of various functional groups common for the three oxidants such as carboxylic, lactonic, phenolic and carbonyl groups. But the intensity of IR absorption peaks is modified depending of the oxidizing agent, being that effect more important for nitric acid oxidation [9-14, 16, 17].

Depending on the ability of the oxidizing agent to diffuse into the carbon pores, the surface groups introduced seem to be preferentially located on the external or non-microporous surface upon oxidation with H_2O_2 and $(\text{NH}_4)_2\text{S}_2\text{O}_8$ while nitric acid oxidation creates more oxygen complexes on the internal surface of the carbon particles [9, 12, 16, 17]. This could be linked to a higher erosion of the particle surface that facilitates the access of nitric acid [11, 12, 17].

The aim of this work is to explore the preparation of activated carbon from grape seeds char by cyclic liquid phase oxidation and desorption. The influence of the type of oxidizing agent, the desorption temperature and the number of cycles applied is studied in order to achieve a convenient development of porosity at low burn-off, so that the morphology of the char is preserved as well as its physical integrity.

2. Materials and methods

The raw material used in this study consisted of seeds collected from grapes of the red variety “Tinta de Toro” harvested for red wine manufacture in Toro (Zamora, Spain). The seeds were washed, dried and then extracted with hexane to remove essential oil before pyrolysis [18]. The oil content of grape seeds depends on the grape variety, though usually ranges around 10-16% weight on a dry basis [19]. In our case it amounted 9%. The char used as starting material was obtained by flash pyrolysis of the extracted seeds at 800°C, as reported in a previous work [18]. The char yield was 34% of the extracted seeds weight on a dry basis.

2.1 Samples characterization

Surface area and total pore volume of the carbon samples were measured in an automated volumetric gas adsorption Micromeritics apparatus (Tristar 3020) by adsorption of N₂ at 77K, and CO₂ at 273K. Approximately 0.15g of sample were used in each test which were placed in a glass container and degassed at 150°C for 7h at atmospheric pressure prior to the adsorption measurements, using a Micromeritics sample degas system (VacPrep 061). Samples were kept in dry atmosphere immediately after pyrolysis and activation. The apparent surface area was calculated from the N₂ isotherm using the Brunauer-Emmett-Teller (BET) equation (S_{BET}) [20], the t-method was used for the micropore volume and BJH method was used to obtain the narrow and total mesopore volume and the mean mesopore size, whereas Dubinin-Astakhov (DA) model (with an equation exponent value of 2) was applied to the CO₂ isotherms obtained in the $10^{-5} - 0.03 P/P_0$ range, to determine the DA surface area (S_{DA}) and

micropore volume [21]. The area S_{DA} was used here as an apparent surface area for comparative purposes since it is based on volume filling. Mercury intrusion porosimetry was used to determine the macropore volume (V_{macro}). The Non-Local Density Functional Theory (DFT) method was used to calculate the pore size distribution [22].

Fourier transform infrared spectroscopy (FTIR) was used to characterize the main functional groups of the activated carbons surface using a spectrometer FTIR Bruker IFS66v connected to a MCT detector whose spectral measurement range goes from 7000 to 550 cm^{-1} .

The morphology of grape seeds char and activated carbons was analyzed by Scanning Electron Microscopy (SEM), using a Hitachi S-3000N apparatus. The specimens for SEM observation were metalized with gold to prevent electrical charging during examination using a Sputter Coater SC502. Imaging was done in the high vacuum mode under an accelerating voltage of 20kV, using secondary electrons.

2.2 Cyclic activation

The procedure followed for the oxidation step was different depending on the oxidizing agent. Oxidation with 30% HNO_3 was carried out by boiling under reflux for 20min. Oxidation with 30% H_2O_2 and 1M $(NH_4)_2S_2O_8$ was performed at 20°C for 24h under stirring. After oxidation the samples were washed with distilled water until neutrality and dried in a muffle at 105°C. These conditions are reported in the literature as commonly used to effectively oxidize the surface of carbons for different applications [7, 12].

The desorption step was carried out in a vertical quartz tube (70cm length and 3.5cm internal diameter) placed in a clam-shell electrical furnace at 850°C and 950°C for 2h using a flow rate of 100mLmin⁻¹ of nitrogen and a heating rate of 10°Cmin⁻¹. These desorption conditions were established according to previous works [2, 4, 5]. After each activation cycle the reactor was cooled under nitrogen flow, the activated carbon was collected, and the yield and textural properties were determined before starting a new cycle.

The activated carbons were designated by the activating agent, desorption temperature and the number of cycles applied, e.g. for sample H₂O₂-850 C1, oxidation was carried out with H₂O₂ at 850°C desorption temperature and 1 activation cycle was completed.

3. Results and discussion

Under all the combinations of oxidizing agent and desorption temperature tested, the burn-off increased almost linearly with the number of activation cycles applied (Figure 1). Likewise, burn-off showed, as a general trend, an increase with desorption temperature. The highest burn-off values were observed for the activated carbon series prepared with HNO₃, and the lowest for the H₂O₂ one.

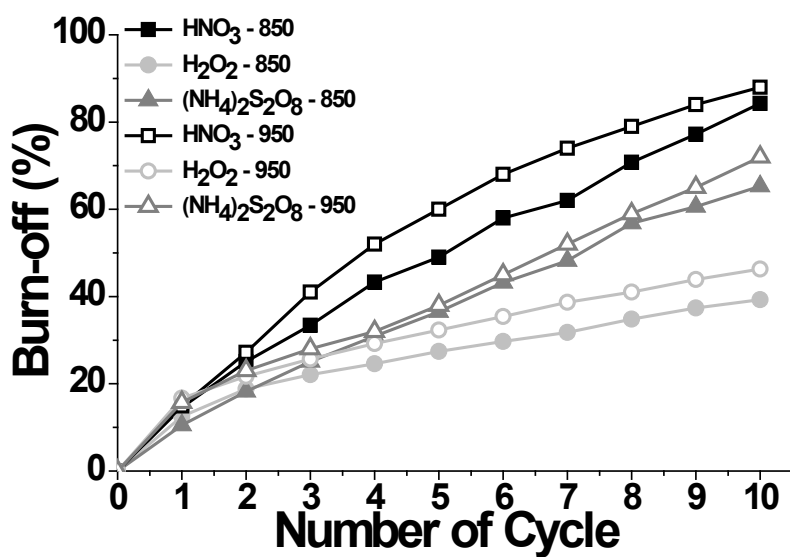


Figure 1. Burn-off vs number of activation cycles with different oxidizing agents and desorption temperatures.

The nitrogen adsorption-desorption isotherms of the starting char and the activated carbons resulting after five activation cycles are shown in Figure 2. The activated carbons yielded isotherms representative of essentially microporous solids with low contribution of mesoporosity, which increases for the samples with higher burn-off as suggested by a more rounded knee and a somewhat higher slope of the plateau-like region. The existence of slight hysteresis loops confirms the low extent of mesopore development.

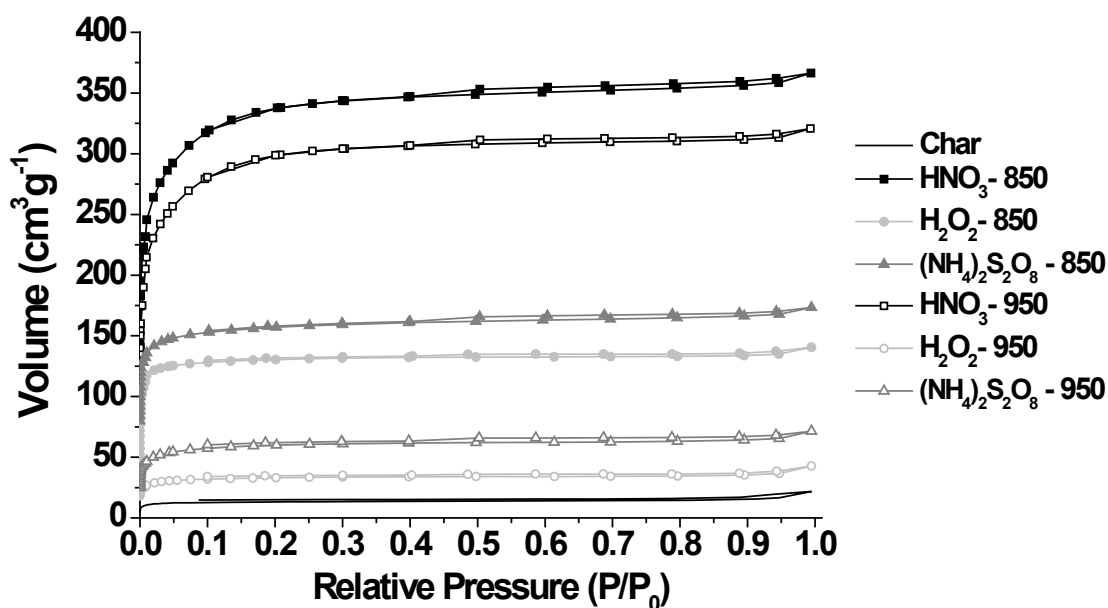


Figure 2. 77K N₂ adsorption-desorption isotherms of grape seed char and activated carbons after five activation cycles.

The starting char used in this work was essentially microporous with a S_{BET} of $47\text{m}^2\text{g}^{-1}$ and a S_{DA} of $505\text{m}^2\text{g}^{-1}$ [18]. The low BET surface area determined using nitrogen compared to that of CO₂ can be explained due to limited diffusion of the N₂ molecule at 77K into narrow pores unlike the CO₂ result at 273K which has no difficulty of progressing into the narrow pores at the much higher analysis temperature. Thus, the development of porosity of the resulting activated carbons was evaluated not only by the BET method but also by the Dubinin-Astakhov one. The Dubinin-Radushkevich and Dubinin-Astakhov equations have been used to explain the filling of micropores and the energetic heterogeneity of porous solids. But while some studies [23, 24] postulated that the Dubinin-Radushkevich equation applies only to solids with a uniform structure of micropores, others [25-29] propose a modification for microporous solids of distributed

size. One of them is the well-known Dubinin-Astakhov (DA) equation, which can be used to describe adsorption on solids with a heterogeneous microporosity [21, 30].

Figure 3 shows the development of surface area with the number of activation cycles. It can be seen that a desorption temperature of 850°C leads to a S_{BET} development upon the first cycles higher than the observed at 950°C, in spite of the higher burn-off values achieved at this second temperature. This may be related with thermal stress leading to partial collapse of the microporous structure [31]. In the case of HNO_3 the development of porosity per cycle remained high up to the 5th-6th cycle, reaching S_{BET} values above 1200 m²g⁻¹. Beyond that the increase of S_{BET} was slower, due to the coalescence of pores associated to high burn-off. Likewise, increasing the number of cycles decreases the differences in S_{BET} between the series of activated carbons prepared at the two desorption temperatures tested. After 10 activation cycles with HNO_3 a S_{BET} value around 1450 m²g⁻¹ was achieved.

With $(\text{NH}_4)_2\text{S}_2\text{O}_8$ and H_2O_2 as oxidizing agents, the development of S_{BET} was substantially lower, particularly when the desorption stage was carried out at 950°C where the creation of S_{BET} was of low significance upon the five first cycles. The lowest S_{BET} development was observed for the H_2O_2 series, with S_{BET} values below 600 m²g⁻¹ after 10 activation cycles.

The evolution of S_{DA} shows higher values than S_{BET} during the first activation cycles, indicating a predominantly narrow microporosity of the resulting carbons. As burn-off increases new narrow microporosity is created and widening of existing pores takes place, being that more evident in the nitric acid series. With H_2O_2 , the S_{BET} after ten

activation cycles is still lower than $600\text{m}^2\text{g}^{-1}$ and remains below S_{DA} , particularly at a desorption temperature of 950°C .

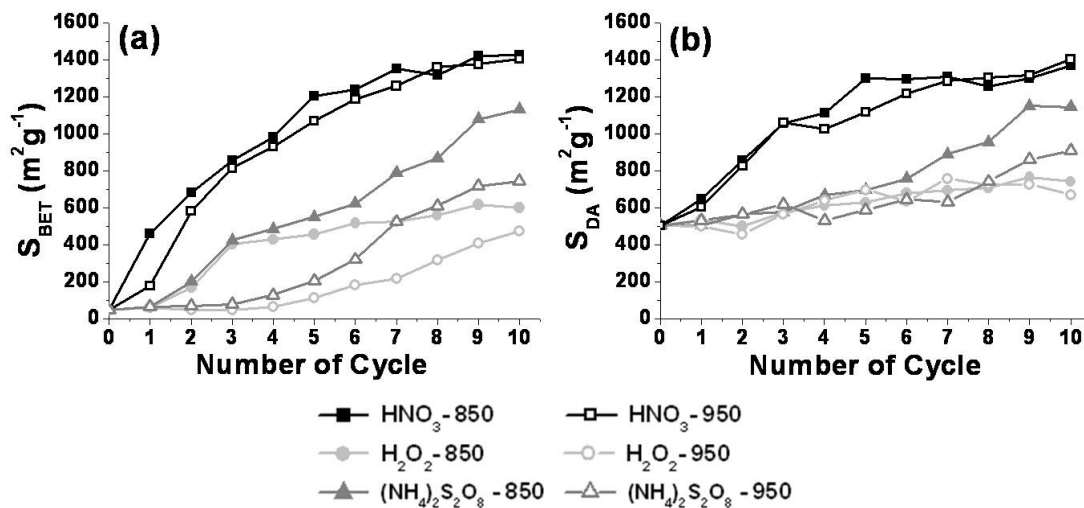


Figure 3. S_{BET} (a) and S_{DA} (b) development upon successive activation cycles.

Convenient operating conditions can be established in 5 activation cycles and a desorption temperature of 850°C for the HNO_3 series, leading to activated carbons with S_{BET} close to $1200\text{m}^2\text{g}^{-1}$ at burn-off lower than 50%. The generation of high surface area at as low burn-off as possible is crucial for the sake of preserving the physical integrity of the particles so that granular activated carbon can be obtained. For the $(\text{NH}_4)_2\text{S}_2\text{O}_8$ series around 8 cycles would be needed to obtain S_{BET} values close to $900\text{m}^2\text{g}^{-1}$ at a burn-off ca. 55%. More modest values of surface area are obtained in the case of the H_2O_2 series, although these activated carbons can be of interest thanks to their pore size distribution with a predominantly narrow microporosity as can be inferred from the comparison of the S_{BET} and S_{DA} values of Figure 3. Thus, those activated carbons may have potential application as molecular sieves.

As can be observed in Figure 4, very low mesopore volume was achieved under all the activation conditions tested, in contrast with the important development of

microporosity occurred from the first activation cycle. An incipient development of mesopores can be observed from the first cycle for the HNO_3 series, and from the fourth cycle for the $(\text{NH}_4)_2\text{S}_2\text{O}_8$ one. That fairly modest generation of mesoporosity must be due to the widening of previously created micropores [11], as it was mentioned before. The development of mesopores was observed once the activated carbons achieved a micropore volume of around $0.25\text{cm}^3\text{g}^{-1}$. It is remarkable that after 10 activation cycles the $\text{HNO}_3 - 850\text{ C10}$ sample showed quite a high micropore volume ($0.69\text{cm}^3\text{g}^{-1}$) with a relatively low mesopore one ($0.067\text{cm}^3\text{g}^{-1}$). The carbons with a less developed porosity, i.e. the H_2O_2 series, show an almost negligible contribution of mesopores (around $0.01\text{cm}^3\text{g}^{-1}$ at the most) which reinforces the aforementioned potential interest as molecular sieves, although further studies will be needed to check this.

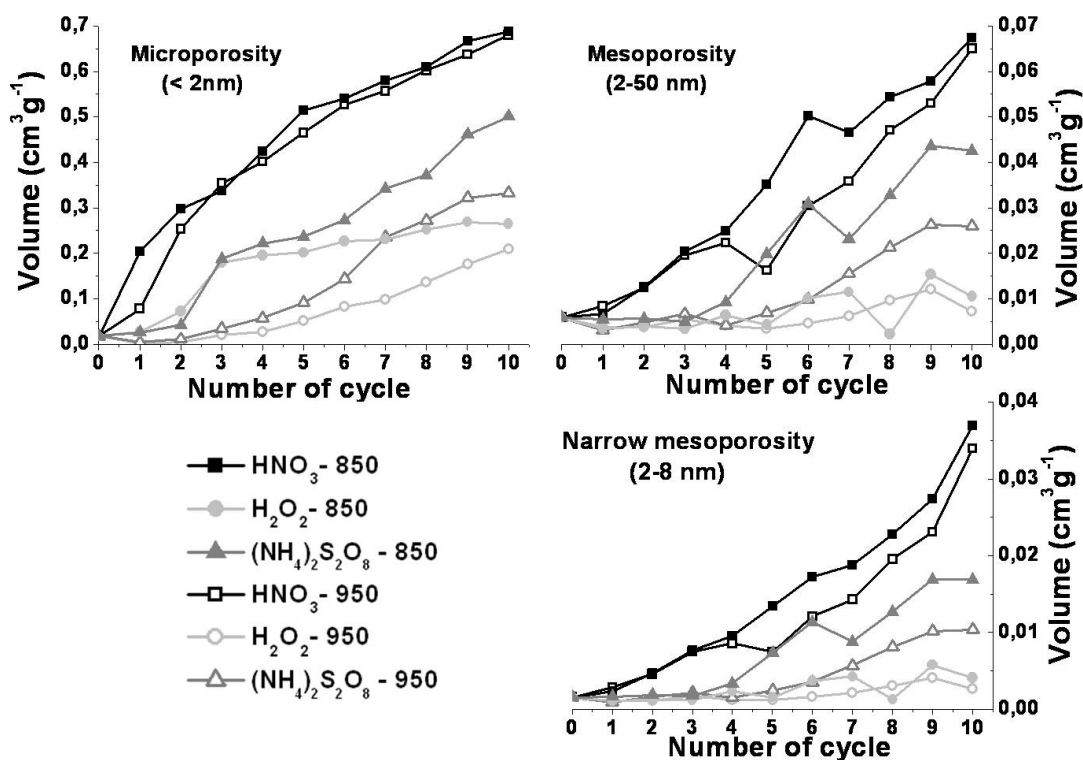


Figure 4. Pore volume development from N₂ adsorption isotherms along the cycles for different oxidizing agents and desorption temperatures.

To learn more in depth on the porous structure of these carbons, their pore size distribution (PSD) was obtained. As a first approach Figure 5 shows that the mean micropore size increases with the number of activation cycles (and, consequently burn-off), while the mean mesopore size decreases. The decrease in mean mesopore size can be ascribed to the formation of narrow mesopores by coalescence of micropores upon burn-off. At burn-off values above 50% the mean mesopore size becomes quite similar for all the carbons obtained, approaching to 2nm, the upper limit of micropores.

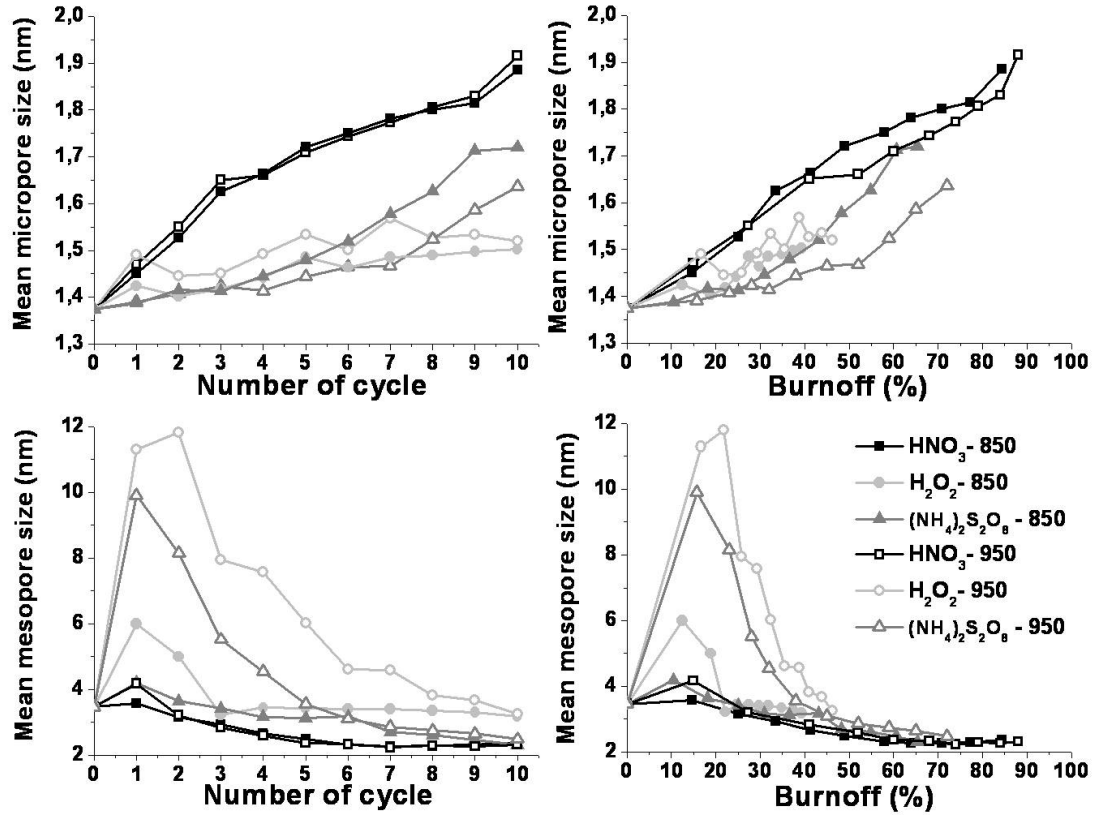


Figure 5. Mean micropore size from CO₂ isotherms and mean mesopore size from N₂ isotherms versus number of cycles and burn-off.

The non-local density functional theory (NLDFT) is widely used for the characterization of the porous structure of activated carbons and other porous materials [22]. In Figure 6 the micropore and mesopore size distributions calculated by the NLDFT method from CO₂ and N₂ adsorption, respectively, are depicted for three selected carbons (one of each series) obtained at similar values of burn-off (around 40%). As can be observed, the CO₂-NLDFT distribution is very similar for the three samples and falls essentially within the micropore range in agreement with the nature of the porosity of these carbons so far discussed. Their PSD seems to be determined in some extent by that of the starting char within the micropore range. On the contrary in

the mesopore range there are clear differences between the sample activated with HNO_3 and the two other, particularly looking at the narrower mesopores (below 3nm). No significant differences can be found in the pattern of mesoporosity within the 8-50nm range, being this porosity initially present in the starting char. Summarizing, the activated carbons of essentially microporous nature have a heterogeneous micropore size distribution centered at 0.45, 0.55 and 0.88nm.

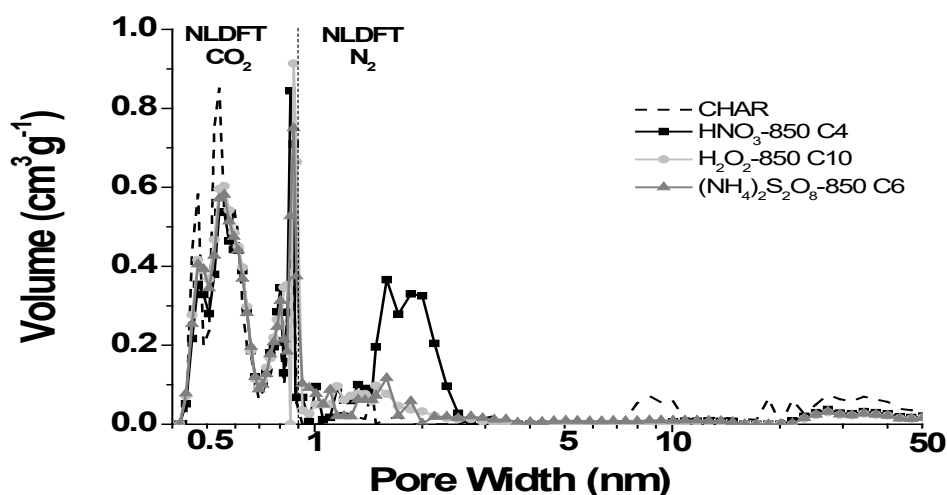


Figure 6. Pore size distribution by NLDFT method from CO_2 and N_2 isotherms for selected carbon samples.

Table 1 shows the macropore volume obtained from mercury porosimetry of the activated carbons prepared at desorption temperature of 850°C after 5 and 10 activation cycles. As can be seen, the number of oxidation/desorption cycles and the oxidizing agent also have a significant effect on the macroporosity of the resulting carbons. The macropore volume increases with the number of cycles applied and with burn-off being appreciably higher in the HNO_3 series [32].

Table 1. Macropore volume from mercury porosimetry between 0.01 and 4 μ m after 5 and 10 activation cycles.

	$V_{\text{macro}}(\text{cm}^3\text{g}^{-1})$		
	$\text{H}_2\text{O}_2\text{-850}$	$(\text{NH}_4)_2\text{S}_2\text{O}_8\text{-850}$	$\text{HNO}_3\text{-850}$
Char	0.707		
Cycle 5	0.293	0.309	0.347
Cycle 10	0.386	0.455	0.551

Fourier transform infrared spectroscopy (FTIR) was used for the characterization of the main functional groups of the activated carbons surface. The spectra for the three series (Figure 7) were quite similar, showing essentially the same main peaks although with different intensities that increase with the number of cycles, so it can be interpreted in terms of progressive increase of the type and quantity of functional groups on the surface of the activated carbons. Therefore, the desorption at high temperature does not remove all the surface oxygen groups created upon oxidation and the most heat-resistant groups build up on the activated carbon surface. The overlapping of bands in the 1300 to 900 cm^{-1} range probe the presence of C—O bonds in various chemical surroundings, where $\gamma(\text{O—H})$ vibrations in ring ethers and primary C—OH occur [33, 34]. Likewise, bands in the vicinity of 1350 cm^{-1} ascribable to $\delta(\text{O—H})$ and $\gamma(\text{C=O})$ vibrations. Relevant bands can also be found around 3600 cm^{-1} , assessed to non-bonded OH groups, and at 3225 and 3350 cm^{-1} , which correspond to $\gamma(\text{O—H})$ vibrations in hydroxyl groups. Olefinic $\gamma(\text{C=C})$ vibrations and skeletal C=C vibrations in aromatic rings can be responsible for the overlapping of bands in the 1700-1400 cm^{-1} range [33].

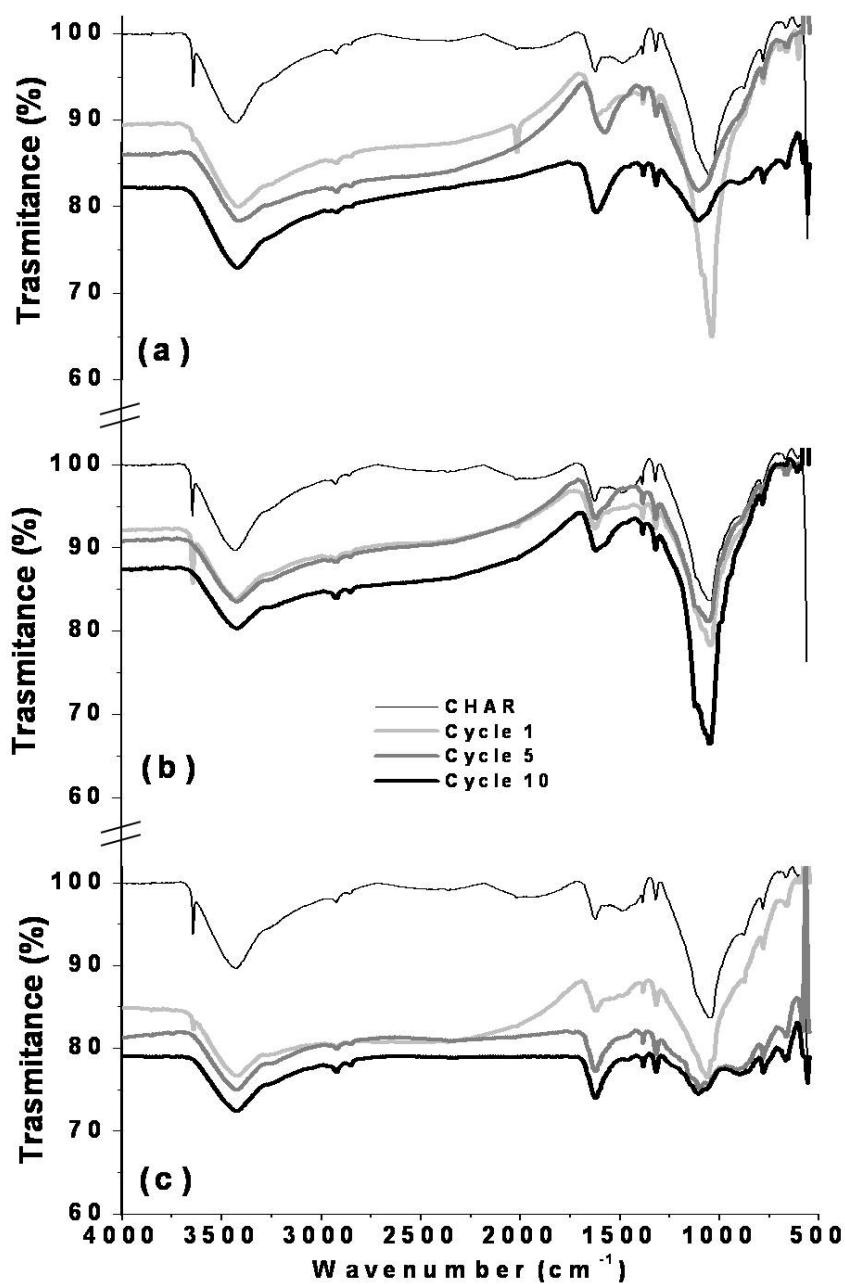


Figure 7. FTIR spectra of (a) HNO₃-850 series, (b) H₂O₂-850 series, (c) (NH₄)₂S₂O₈ - 850 series.

3.1 Morphological analysis

The morphology of the activated carbons was evaluated by SEM, showing that the granular structure was maintained along the cycles independently of the oxidizing agent

used (Figure 8). Furthermore, there is also a reduction in size with respect to that of the starting seed along the cycles. It can also be observed that the samples activated with H_2O_2 and $(\text{NH}_4)_2\text{S}_2\text{O}_8$ have a higher prevalence of cracks on the outer surface.

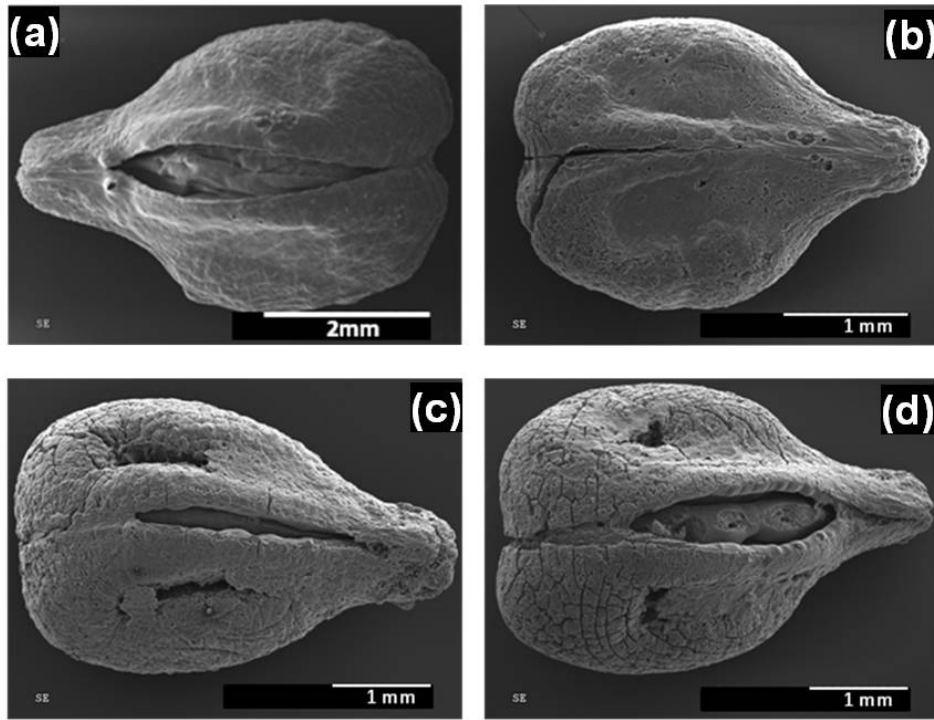


Figure 8. SEM micrographs of (a) char from grape seed (b) HNO_3 - 850 C10 sample (c) H_2O_2 - 850 C10 sample (d) $(\text{NH}_4)_2\text{S}_2\text{O}_8$ - 850 C10 sample.

Figure 9 shows SEM images of crushed particles showing the hollow core structure of the carbon particles after 10 activation cycles with HNO_3 as activating agent. The hollow structure results from the volatilization of the albumen and embryo during the pyrolysis stage and is maintained along the activation. The activated carbon has most of the carbonaceous material allocated in a shell thickness of around $300\mu\text{m}$, being that an interesting feature since the granular material would combine easy handling and low

pressure loss for packed bed applications with a convenient structure as adsorbent due to short diffusion path [35].

It can be observed that after 10 activation cycles both the outer layer and the carbonized tissue in the inner of the particle have been partially removed compared to the char (see SEM images of Figures 9 and 10). Likewise, a more open structure can be observed, in agreement with the larger volume of macropores determined by mercury porosimetry (Table 1). Such macropores can act as convenient channels for diffusion in adsorption applications.

The packed bed bulk density was calculated for the starting char and the activated carbons obtained after ten cycles of activation with HNO_3 , $(\text{NH}_4)_2\text{S}_2\text{O}_8$ and H_2O_2 , the values being 0.26, 0.16, 0.18 and 0.25 g/cm^3 , respectively. The density decreases with burn-off, particularly for the activation with HNO_3 and $(\text{NH}_4)_2\text{S}_2\text{O}_8$, although the values obtained do not indicate a drawback provided that there are not equipment size limitations.

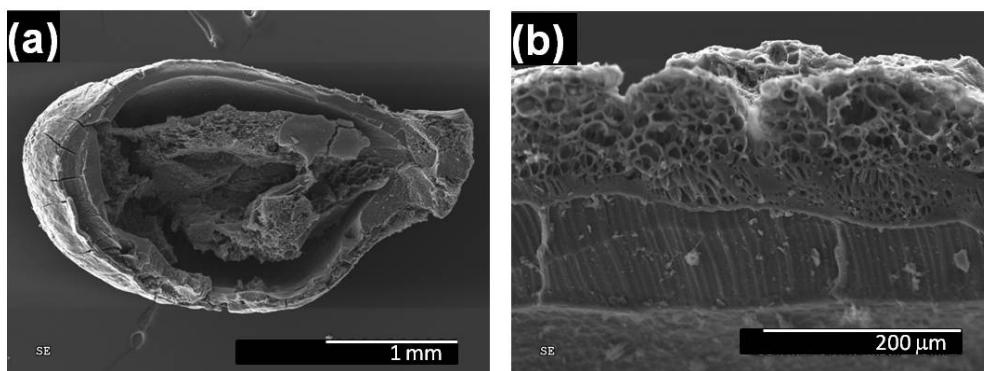


Figure 9. (a) Cross section and (b) Detail of wall of HNO_3 - 850 C10 sample.

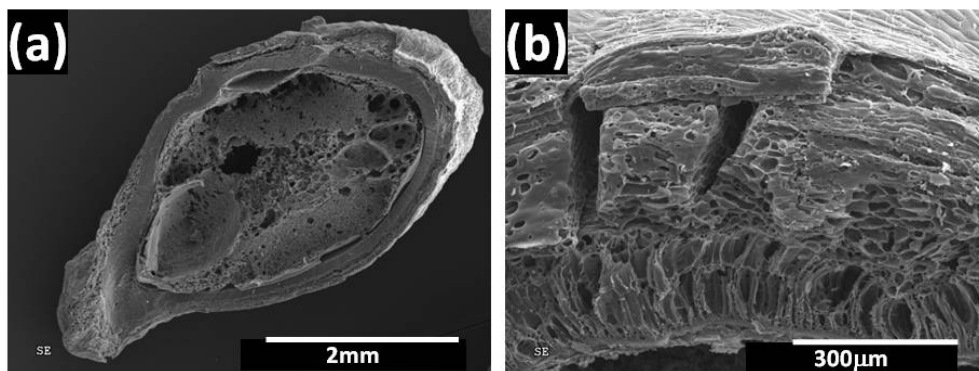


Figure 10. a) Cross section of a grape seed char. b) Carbonized seed coat (char).

4. Conclusions

Activation of grape seed char upon successive cycles of liquid-phase oxidation followed by high temperature desorption has demonstrated its potential interest for the preparation of granular activated carbon. The procedure proposed permits a controlled development of porosity.

The burn-off increased almost linearly with the number of activation cycles, with a burn-off per cycle increasing in the following order: $\text{HNO}_3 > (\text{NH}_4)_2\text{S}_2\text{O}_8 > \text{H}_2\text{O}_2$. The burn-off was also higher for the activated carbons prepared at a desorption temperature of 950°C .

HNO_3 was found to be more efficient for the development of porosity, in terms of surface area per unit of burn-off, whereas no relevant differences were found between $(\text{NH}_4)_2\text{S}_2\text{O}_8$ and H_2O_2 . The efficiency was higher at 850°C desorption temperature. The activation process led to the development of porosity essentially in the micropore range with a very low contribution of mesoporosity. Activation with H_2O_2 led to carbons with a predominantly narrow microporosity even after ten activation cycles.

Convenient selection of the activation conditions makes possible tailoring the activated carbon porosity and pore size distribution. Carbons with S_{BET} values up to around $1400\text{m}^2\text{g}^{-1}$ with $0.69\text{cm}^3\text{g}^{-1}$ of micropore volume and a small volume ($0.07\text{cm}^3\text{g}^{-1}$) of narrow mesopores were prepared by activation with HNO_3 . With $(\text{NH}_4)_2\text{S}_2\text{O}_8$ and H_2O_2 were obtained activated carbons with S_{BET} values up to 1100 and $600\text{m}^2\text{g}^{-1}$ respectively, mean micropore size below 1.5nm and very low mesopore contribution, even lower than 0.045 and $0.01\text{cm}^3\text{g}^{-1}$ respectively.

The activated carbons prepared maintain the initial morphology of the grape seed chars thanks to the low burn-off needed for convenient porosity development, showing a hollow core structure with a wall thickness around $200\mu\text{m}$. Such structure is of interest for adsorption applications due to low diffusion path.

5. Acknowledgment.

The authors greatly appreciate financial support from the Spanish Ministerio de Ciencia e Innovación (CTQ2009-09983).

6. References

- [1] X. Py, A. Guillet, B. Cagnon. *Activated carbon porosity tailoring by cyclic sorption/decomposition of molecular oxygen*. Carbon 41 (2003) 1533-1543.
- [2] F. Heras, N. Alonso-Morales, D. Jiménez-Cordero, M.A. Gilarranz, J.J. Rodríguez. *Granular mesoporous activated carbons from waste tires by cyclic oxygen chemisorption-desorption*. Ind. Eng. Chem. Res. 51 (2012) 2609-2614.
- [3] D.F. Quinn, J.A. Holland. *Carbonaceous material with high micropore and low macropore volumen and process for producing same*. US Pattenet 5,071,820 (1991)

- [4] F. Heras, N. Alonso, M.A. Gilarranz, J.J. Rodríguez. *Activation of waste tire char upon cyclic oxygen chemisorption-desorption*. Ind. Eng. Chem. Res. 48 (2009) 4664 – 4670.
- [5] D. Jiménez-Cordero, F. Heras, N. Alonso-Morales, M.A. Gilarranz, J.J. Rodríguez. *Development of porosity upon physical activation of grape seeds by gas phase oxygen chemisorption-desorption cycles*. Chem. Eng. J. (2013) doi: 10.1016/j.cej.2013.07.005.
- [6] F. Heras, D. Jiménez, N. Alonso, M.A. Gilarranz, J.J. Rodríguez. *Liquid phase oxidation for the activation of waste tyres char by cyclic oxidation/desorption*. International Conference on Carbon, Shanghai (China) 24/07/2011 – 29/07/2011.
- [7] R. Mysyk, Q. Gao, E. Raymundo-Piñero, F. Béguin. *Microporous carbons finely-tuned by cyclic high pressure low-temperature oxidation and their use in electrochemical capacitors*. Carbon 50 (2012) 3367-3374.
- [8] J.S. Noh, J.A. Schwart. *Effect of HNO₃ treatment on the surface acidity of activated carbons*. Carbon 28 (1990) 675-682.
- [9] L. Calvo, M.A. Gilarranz, J.A. Casas, A.F. Mohedano, J.J. Rodríguez. *Hydrodechlorination of 4-chlorophenol in aqueous phase using Pd/AC catalysts prepared with modified active carbon supports*. Appl. Catal. B-Environ. 67 (2006). 68-76.
- [10] J.L. Figueredo, M.F.R. Pereira, M.M.A. Freitas, J.J.M. Órfao. *Modification of the surface chemistry of activated carbons*. Carbon 37 (1999) 1379-1389.
- [11] A-NA El-Hendawy. *Influence of HNO₃ oxidation on the structure and adsorptive properties of corncob-based activated carbon*. Carbon 41 (2003) 713-722.
- [12] X. Lu, J. Jiang, K. Sun, X. Xie, Y. Hu. *Surface modification, characterization and adsorptive properties of a coconut activated carbon*. Appl. Surf. Sci. 258 (2012) 8247–8252.
- [13] M. Belhachemi, R.V.R.A. Rios, F. Addoun, J. Silvestre-Albero. A. Sepúlveda-Escribano, F. Rodríguez-Reinoso. *Preparation of activated carbon from date pits: Effect of the activation agent and liquid phase oxidation*. J. Anal. Appl. Pyrolysis 86 (2009) 168-172.

- [14] J. Jaramillo, P. Modesto Álvarez, V. Gómez-Serrano. *Oxidation of activated carbon by dry and wet methods surface chemistry and textural modifications*. Fuel Process. Technol. 91 (2010) 1768-1775.
- [15] A. Gil, G. de la Puente, P. Grange. *Evidence of textural modifications of an activated carbon on liquid-phase oxidation treatments*. Microporous Mater. 12 (1997) 51-61.
- [16] X. Song, H. Liu, L. Cheng, Y. Qu. *Surface modification of coconut-based activated carbon by liquid-phase oxidation and its effects on lead ion adsorption*. Desalination 255 (2010) 78-83.
- [17] C. Moreno-Castilla, M.V. López-Ramón, F. Carrasco-Marín. *Changes in surface chemistry of activated carbons by wet oxidation*. Carbon 38 (2000) 1995-2001.
- [18] D. Jiménez-Cordero, F. Heras, N. Alonso-Morales, M.A. Gilarranz, J.J. Rodríguez. *Porous structure and morphology of granular chars from flash and conventional pyrolysis of grape seeds*. Biomass Bioenergy 54 (2013) 123-132.
- [19] A. Molero Gómez, C. Pereyra López, E. Martínez de la Ossa. *Recovery of grape seed oil by liquid and supercritical carbon dioxide extraction: a comparison with conventional solvent extraction*. Chem. Eng. J. 61 (1996) 227-231.
- [20] S. Brunauer, E. Emmett, E. Teller. *Adsorption of gases in multimolecular layers*. Amer. Chem. Soc. J. 60 (1938) 309-319.
- [21] A. Gil, P. Grange. *Application of the Dubinin-Radushkevich and Dubinin-Astakhov equations in the characterization of microporous solids*. Coll. Surf. A: Physicochem. Eng. Asp. 113 (1996) 39-50.
- [22] J. Jagiello, M. Thommes. *Comparison of DFT characterization methods based on N₂, Ar, CO₂ and H₂ adsorption applied to carbons with various pore size distributions*. Carbon 42 (2004) 1227-1232.
- [23] H.F. Stoeckli. *A generalization of the Dubinin—Radushkevich equation for the filling of heterogeneous micropore systems*. J. Coll. Int. Sci. 59 (1977) 184–185.
- [24] M. Jaroniec, J. Piotrowska. *Isotherm equations for adsorption on heterogeneous microporous solids*. Monatsh. Chem. 117 (1986) 7-19.

- [25] A. Gil, M. Montes. *Analysis of the microporosity in pillared clays*. Langmuir 10 (1994) 291-297.
- [26] M. Jaroniec, J. Choma. *On the characterization of structural heterogeneity of microporous solids by discrete and continuous micropore distribution functions*. Mater. Chem. Phys. 19 (1988) 267-289.
- [27] M.M. Dubinin. *Inhomogeneous microporous structures of carbonaceous adsorbents*. Carbon 19 (1981) 321-324.
- [28] M. Rodwadowski, R. Wojsz. *An attempt at determination of the structural heterogeneity of microporous adsorbents*. Carbon 22 (1984) 363-367.
- [29] M. Jaroniec, R.K. Gilpin, K. Kaneko. *Evaluation of energetic heterogeneity and microporosity of activated carbon-fibers on the basis of gas-adsorption isotherms*. Langmuir 7 (1991) 2719-2722.
- [30] M. Carrasco-Marin, M.V. Lopez-Ramon, C. Moreno-Castilla. *Applicability of the Dubinin-Radushkevich equation to carbon dioxide adsorption on activated carbons*. Langmuir 9 (1993) 2758-2760.
- [31] M. Polyakov, M. Poisot, W.E. Maurits, T. Drescher, A. Lotnik, L. Kienle, W. Bensch, M. Muhler, W. Grunert. *Carbon-stabilized mesoporous MoS₂ - Structural and surface characterization with spectroscopic and catalytic tools*. Catal. Commun. 12 (2010) 231-237.
- [32] W.M.A.W. Daud, W.S.W. Ali. *Comparison on pore development of activated carbon produced from palm shell and coconut shell*. Bioresour. Technol. 93 (2004) 63 – 69.
- [33] P.M. Álvarez, J.F. García-Araya, F.J. Beltrán, F.J. Masa, F. Medina. *Ozonation of activated carbons: Effect on the adsorption of selected phenolic compounds from aqueous solutions*. J. Coll. Int. Sci. 283 (2005) 503-512.
- [34] L. Stobinski, B. Lesiak, L. Kövér, J. Tóth, S. Biniak, G. Trykowski, J. Judek. *Multiwall carbon nanotubes purification and oxidation by nitric acid studied by the FTIR and electron spectroscopy methods*. J. Alloys Comp. 501 (2010) 77-84.

[35] M.J. Prauchner, F. Rodriguez-Reinoso. *Chemical versus physical activation of coconut shell: A comparative study*. Micro. Meso. Mater. 152 (2012) 163-171.